Heliyon 10 (2024) e37171

Contents lists available at ScienceDirect

Heliyon

journal homepage: www.cell.com/heliyon

Research article

Single G-quadruplex-based fluorescence method for the uracil-DNA glycosylase inhibitor screening

Pansong Zhang *, Fangfang He, Xin Chang

Center for Healthy Aging, Changzhi Medical College, Changzhi 046000, Shanxi, PR China

ARTICLE INFO

Keywords:
Uracil-DNA glycosylase
G-quadruplex
UDG inhibitors
Detection

ABSTRACT

Uracil-DNA glycosylase (UDG) plays a pivotal role in the base repair system. Through bioinformatics, we found that the expression of the UDG enzyme in many cancer cells is increased, and its high expression is not conducive to the prognosis of lung cancer patients. The development of analytical techniques for the quantification of UDG activity and the identification of UDG inhibitors is of paramount importance. We found that when the T base in the G4 loop region mutated to uracil, the G4 structure was not disrupted and still retained the characteristics of a G4 structure (emitting strong fluorescence after binding with ThT (Thioflavin T). Inspired by this phenomenon, we developed a detection method for UDG and its inhibitors utilizing a single DNA strand engineered to form a G-quadruplex structure, containing uracil residues within the loop region, designated as G4-dU. The inclusion of uracil-DNA glycosylase (UDG) in the assay environment induces the removal of uracil, resulting in the formation of apurinic sites (AP) within the G4-dU sequence. Subsequent thermal denaturation leads to strand cleavage at AP sites, precluding the reformation of the G-quadruplex configuration and abrogating fluorescence emission. The detection process in this study can be completed in only 30 min to 1 h, offers a straightforward, expedient, and efficacious modality for assessing UDG activity and UDG inhibitor potency, thereby facilitating the discovery of novel therapeutic agents for cancer treatment.

1. Introduction

The fundamental DNA repair mechanism is essential for preventing genomic alterations [1]. Uracil-DNA glycosylase (UDG) is a crucial enzyme in this process, facilitating the hydrolytic removal of uracil from DNA strands where it has been erroneously incorporated, resulting in the generation of apurinic/apyrimidinic (AP) sites [2]. This process triggers the recruitment of endonuclease IV to remove the AP site and correct the incorrect uracil insertion. Changes in intracellular levels of UDG suggest the presence of pathological conditions, including oncogenesis and hereditary disorders [3], demonstrating the importance of developing methods for quantifying UDG activity.

Moreover, the antimetabolite chemotherapeutic agent, 5-fluorouracil (5-FU), exerts cytotoxicity in many malignancies by impeding thymidylate synthase, thereby promoting the misincorporation of uracil or 5-FU into DNA [4,5]. Nonetheless, therapeutic resistance in cancer patients is frequently attributable to the cellular presence of UDG that excises these erroneous incorporations [6,7]. Thus, identifying small-molecule inhibitors of UDG has emerged as a strategy to potentiate the antineoplastic efficacy of 5-FU [8,9].

In pursuit of UDG activity and inhibitor detection, researchers have focused on the G-quadruplex (G4) fluorescence paradigm.

* Corresponding author.
E-mail address: 15809281696@163.com (P. Zhang).

https://doi.org/10.1016/j.heliyon.2024.e37171
Received 22 April 2024; Received in revised form 12 August 2024; Accepted 28 August 2024
Available online 30 August 2024

Thioflavin T (ThT), which is non-fluorescent when unbound, exhibits pronounced luminescence upon G4 interactions [10,11]. For example, assays have been developed using a primer sequence containing deoxyuridine (dU), which, after UDG-mediated removal and subsequent endonuclease IV activity, generates a primer suitable for binding to a specific substrate. This primer initiates strand displacement amplification (SDA) [12]or rolling circle amplification (RCA) [13], yielding a G4 structure that fluoresces vividly, when complexed with ThT. This can be used to vividly to signal the presence of UDG and to gauge fluorescence attenuation upon UDG inhibitor administration. These methods convert UDG detection into G4 detection via nucleic acid amplification. However, the inclusion of endonucleases associated with strand displacement amplification (SDA) may lead to the non-specific amplification of nucleic acids and false-positive results [14–16]. The RCA design necessitates a protracted circular sequence and a clamping probe, rendering it a more intricate protocol.

In addition, conformational transitions in DNA have been used to isolate UDG inhibitors. This involves two complementary DNA strands, that are dU-rich and guanine-rich, respectively. In the absence of UDG, the strands remain annealed; however, UDG-mediated hydrolysis of dU prompts the transition to a single-stranded DNA and G4 structure [17,18]. The quantification of G4 correlates with UDG activity, facilitating the identificaion of UDG inhibitors, including indole derivatives and the FDA-sanctioned antibiotic nifurazole [19].

Furthermore, RNA sequences that adopted a G4 conformation exhibited enhanced ThT fluorescence upon binding. This phenomenon serves as the basis for the strategy of incorporating deoxyuridine (dU) within the G4 loop, allowing the direct evaluation of UDG activity using ThT fluorescence in the dU-containing G4 sequence, as well as the discovery of UDG inhibitory compounds.

2. Materials and methods

The transcription levels of UDG in pan-cancer and normal cells were analyzed using the Tumor Immunity Estimation Resource (TIMER) database. TIMER database analysis showed that, UNG was significantly elevated in some cancer cells (Table 1), which was verified using the Gene Expression Profiling Interactive Analysis (GEPIA) database. UALCAN (https://ualcan.path.uab.edu/index.html) was used to analyze UNG expression in lung squamous cell carcinoma (LUSC) patients. The Kaplan-Meier Plotter was used to assess the impact of UDG expression on the survival of LUSC patients.

Uracil-DNA glycosylase (UDG), was purchased from Sangon Biotechnology Co., Ltd (Shanghai, China). UGI was acquired from New England Biolabs (Beijing, China). All oligonucleotides were synthesized and purified by Sangon Biotechnology Co., Ltd. (Shanghai, China) and their sequences are listed in Table 2.

2.1. Information retrieval of UDG in different database

The DiffExp module in the TIMER database (https://cistrome.shinyapps.io/timer/) was used to analyze UDG transcription levels in different cancer cells by entering the gene name UNG. GEPIA (http://gepia.cancer-pku.cn/) was used to analyze the transcription levels of genes in a certain cancer by inputting the gene names UNG and cancer names (BLCA, CESC, COAD, DLBC, GBM, LUSC, OV, PAAD, PCPG, READ, TGCT and THYM). UALCAN (https://ualcan.path.uab.edu/index.html) was used to analyze protein expression in patients with certain cancers. The gene name UNG, cancer name LUSC, and other parameters were used at the default values. The Kaplan -Meier Plotter (https://kmplot.com/analysis/) was used to assess the impact of biomarker expression on survival in patients with different types of cancer. The relationship between UNG expression and the prognosis of patients with lung cancer was analyzed using the Kaplan-Meier Plotter. The parameters used were, cancer name = lung cancer and gene name = UNG. Patients were split according to the median, the survival was overall survival (OS) and the follow-up threshold was all.

2.2. UDG detection

10 μL of 1 μM G4-dU probe, a certain concentration of UDG enzyme, and 2 μL of Tris-HCl (1M, pH = 8) was mixed, and water was added to bring the total volume of to 20 μL. The mixture was kept at 37 °C for 1 h, transferred to a metal bath at 95 °C to react for 5–10 min, and immediately placed in an ice bath. After cooling, 15 μL of the solution was taken and combined with 10 μL of 1M KCl, 5 μL of tris-HCl (1M, pH = 8), and 5 μL of 0.5 M ThT, then water was added to reach a final volume of 100 μL. Finally, a microplate reader to was used detect fluorescence intensity. The excitation wavelength was 425 nm, and emission spectra were collected at 455–550 nm.

2.3. Detection of UGI

UDG and UGI were combined in a specific proportion and water was added to reach a volume of 5 μL. 10 μL of 1 μM G4-dU probe, 1 μL of tris-HCl (1M, pH = 8) and 4 μL of ddH_2O were added to 5 μL of the mixture to make 20 μL solution. The mixture was placed at

Table 1
The names of the 12 cancer cells analyzed in the GEPIA database for UDG expression.

BLCA (Bladder Urothelial Carcinoma), CESC (Cervical squamous cell carcinoma and endocervical adenocarcinoma), COAD (Colon adenocarcinoma), DLBC (Lymphoid Neoplasm Diffuse Large B-cell Lymphoma), GBM (Glioblastoma multiforme), LUSC (Lung squamous cell carcinoma), OV (Ovarian serous cystadenocarcinoma), PAAD (Pancreatic adenocarcinoma), PCPG (Pheochromocytoma and Paraganglioma), READ (Rectum adenocarcinoma), TGCT (Testicular Germ Cell Tumors), THYM (Thymoma)

Table 2
The DNA sequences used in this research.

Oligonucleotide	Sequence (5′→3′)
G4-dT	GGGGTTTTGGGGTTTTGGGGTTTTGGGG
G4-dU	GGGGTdUTTGGGGTdUTTGGGGTdUTTGGGG

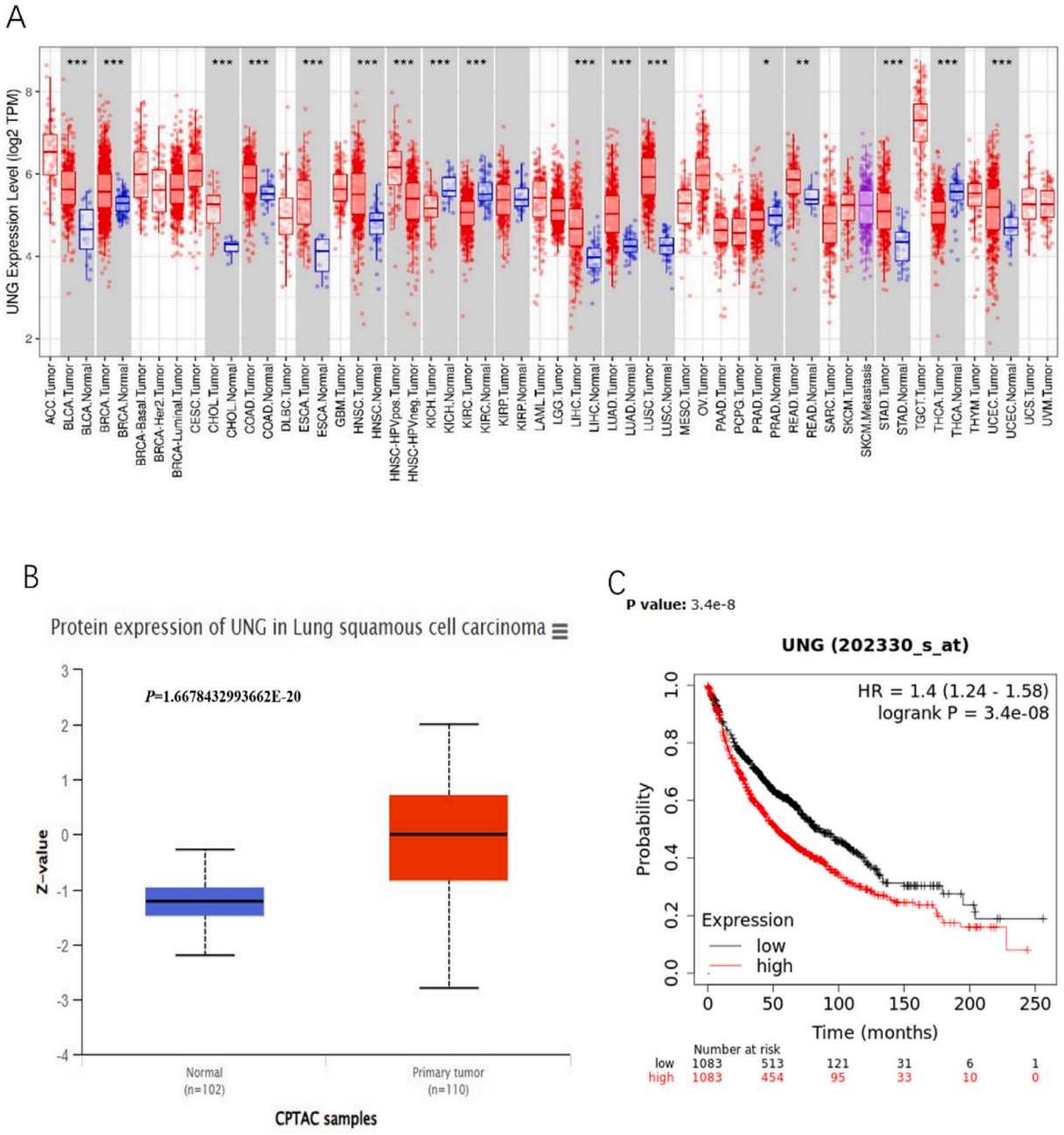

Fig. 1. Analysis of UNG expression levels and their prognostic implications in cance
A. The examination of UNG expression levels across various tumor types utilizing data from the Cancer Genome Atlas (TCGA) database through the Tumor Immune Estimation Resource (TIMER)B. The UNG protein expression in lung cancer and normal tissues was analyzed using the UALCAN database C. The prognostic significance of UNG expression in lung cancer patients as determined by analysis of the Kaplan-Meier Plotter database. *P < 0.05, **P < 0.01, ***P < 0.001.

37 °C for 1h, transferred to a metal bath at 95 °C, reacted for 5–10min, and then immediately cooled. Finally, KCl and ThT were added for fluorescence detection, as described above.

3. Results

3.1. Expression of the UNG enzyme in different tumors

With the advancement of big data and a plethora of omics methodologies, oncological datasets have been aggregated and curated into extensive repositories such as the Cancer Genome Atlas (TCGA). Using the TIMER database, a comprehensive analysis of UNG gene expression was conducted across a spectrum of neoplasms. As illustrated in Fig. 1A, UNG mRNA expression is upregulated in a multitude of cancerous tissues, notably in bladder urothelial carcinoma (BLCA), breast invasive carcinoma (BRCA), cholangiocarcinoma (CHOL), colon adenocarcinoma (COAD), esophageal carcinoma (ESCA), head and neck squamous cell carcinoma (HNSC), liver hepatocellular carcinoma (LIHC), lung adenocarcinoma (LUAD), lung squamous cell carcinoma (LUSC), prostate adenocarcinoma (PRAD), rectal adenocarcinoma (READ), stomach adenocarcinoma (STAD), and uterine corpus endometrial carcinoma (UCEC). Conversely, a downregulation was noted in kidney chromophobe (KICH), kidney clear cell carcinoma (KIRC), and thyroid carcinoma (THCA). Supplementary using via the GEPIA platform corroborated the elevated transcriptional activity of UNG in an expanded panel of neoplasms, including BLCA, cervical squamous cell carcinoma (CESC), COAD, diffuse large B-cell lymphoma (DLBC), glioblastoma multiforme (GBM), LUSC, ovarian cancer (OV), pancreatic adenocarcinoma (PAAD), pheochromocytoma and, paraganglioma (PCPG) rectum adenocarcinoma (READ), testicular germ cell tumors (TGCT), and thymoma (THYM), as shown in Fig. S1. This led to the subsequent determination of UNG mRNA abundance in cancerous cell lines. UALCAN was further incorporated to quantify UNG protein expression in LUSC, with the results shown in Fig. 1B, demonstrating significant overexpression in the LUSC samples. Additionally, the prognostic implications of UNG expression were examined using the Kaplan-Meier Plotter database, focusing on OS in lung cancer cohorts. As shown in Fig. 1C, elevated UNG levels were inversely correlated with patient prognosis in lung cancer, suggesting poorer survival outcomes. Collectively, these bioinformatics inquiries into UNG expression patterns in cancerous pathologies underscore their potential as biomarkers and candidates for diagnostic and therapeutic applications.

3.2. Principle of detecting UDG enzyme activity based on G4-dU structure

In this study, the enzymatic activity of UDG was evaluated using a singular oligonucleotide (G4-dU) capable of adopting a G-quadruplex conformation, as shown in Fig. 2. This oligonucleotide is distinguished by two primary features: its capacity to form a G-quadruplex structure and the substitution of thymine with deoxyuridine within the G4 motif. Upon incubation with ThT, the G4-dU oligonucleotide exhibited a fluorescent response. In contrast, UDG selectively recognizes and excises deoxyuridine from the G4-dU structure to generat apurinic/apyrimidinic (AP) sites. Subsequent treatment of the AP site-containing G4-dU at 95 °C for 10 min induces strand cleavage, thereby causing the formation of the G-quadruplex and extinguishing the fluorescence emission.

3.3. Validation of method feasibility

To ascertain the efficacy of the assay for detecting UDG activity, an initial evaluation was conducted to assess the specific affinity of the G-quadruplex with deoxyuridine (G4-dU) for ThT. The data depicted in Fig. 3A illustrate that the fluorescence emission resulting from the G4-dU/ThT complexation was comparable to that of the G-quadruplex with the deoxythymidine (G4-dT)/ThT interaction. The fluorescence intensity observed for the complexation of G4-dU/ThT was markedly greater than that of the control samples (Fig. 3A

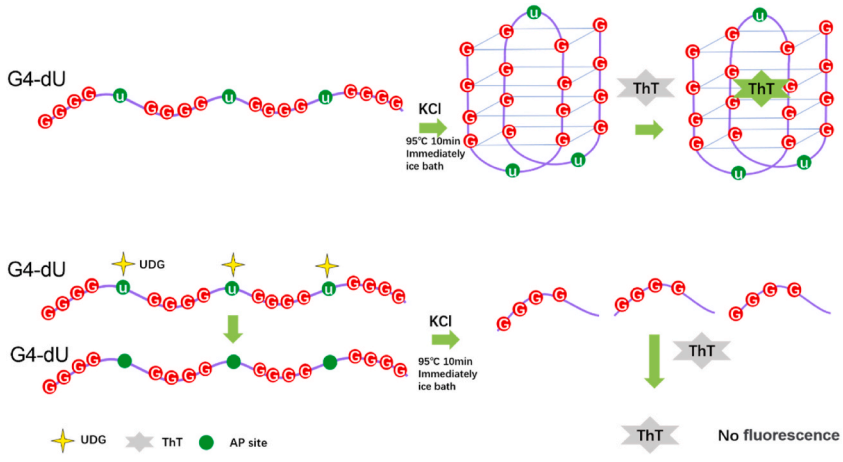

Fig. 2. Schematic representation of the process for detecting uracil-DNA glycosylase (UDG).

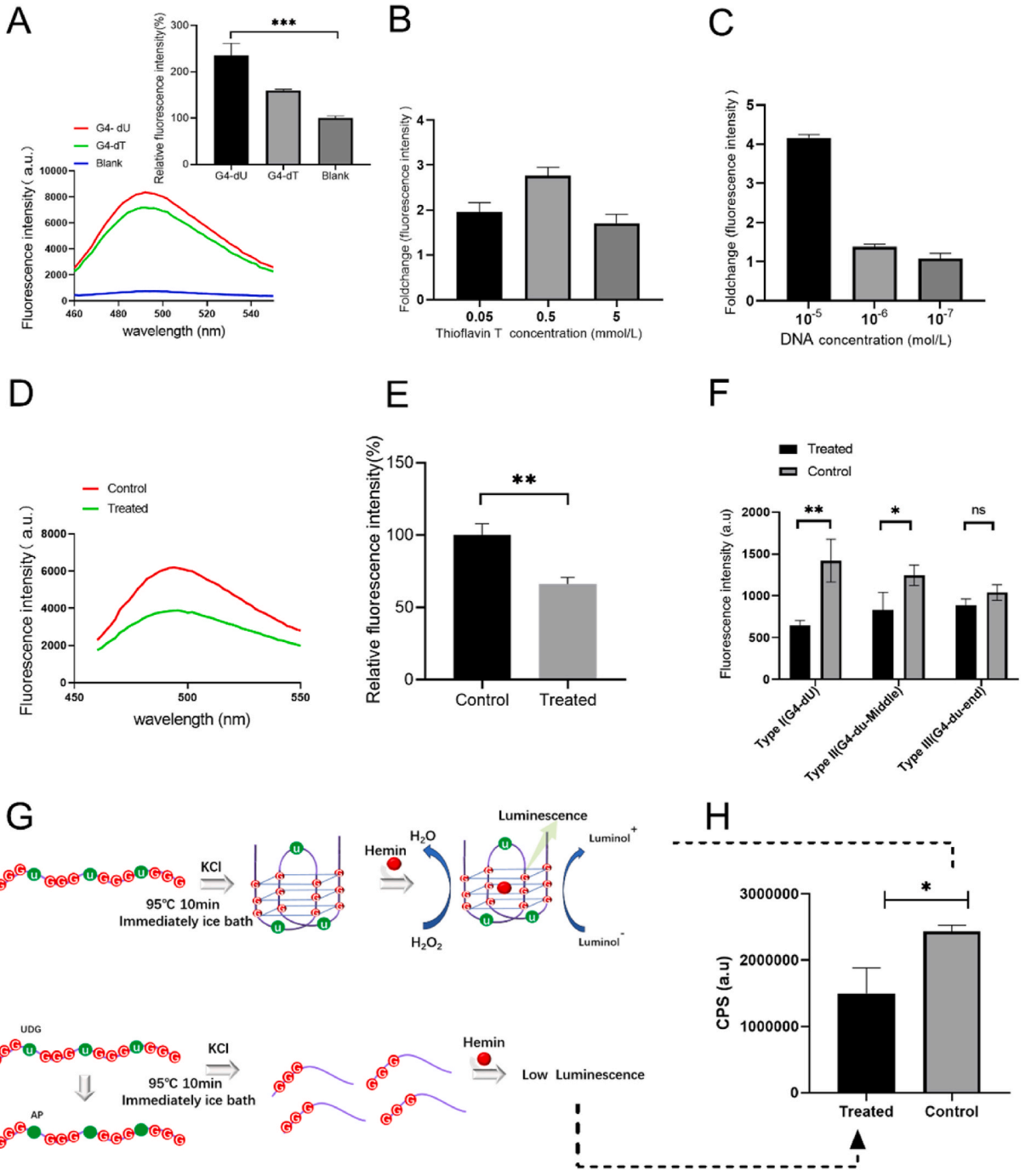

Fig. 3. Validation of the feasibility of the method.

A. Fluorescence emission spectra (a.u.) of ThT in the presence of G4-dT and G4-dU. B. The impact of varying concentrations of ThT on the fluorescence intensity of G4-dU/ThT complexes. C. The impact of varying oligonucleotide concentrations on the fluorescence intensity of G4-dU/ThT complex formation. D. Fluorescence emission mapping of the G4-dU/ThT complex following treatment with uracil-DNA glycosylase (UDG). E. Analysis of the significance of fluorescence intensity in the G4-dU/ThT complex following treatment with uracil-DNA glycosylase (UDG) compared to that of untreated samples. F. Analysis of the fluorescence intensity when ThT binds to various types of G4-dU that have been treated with uracil DNA glycosylase (UDG). Type 1(G4-dU):GGG/ideoxyU//ideoxyU/AGGG/ideoxyU//ideoxyU/AGGG/ideoxyU//ideoxyU/AGGG, Type 2(G4-dU-Middle): GGGTTAGGG/ideoxyU//ideoxyU/AGGGTTAGGG, Type 3(G4-dU-end): GGG/ideoxyU//ideoxyU/AGGGTTAGGGTTAGGG. G. A schematic diagram illustrating the analysis of uracil-DNA glycosylase (UDG) activity through the catalase activity of the G4-dU-Hemin complex. H. Chemiluminescence signals observed following treatment of G4-dU-Hemin complexes with uracil-DNA glycosylase (UDG).

inset).

Concurrently, we investigated the effect of varying the concentrations of ThT (Fig. 3B) and oligonucleotides (Fig. 3C) on the fluorescence intensity of the G4-dU/ThT complex. Based on these findings, subsequent experiments were conducted using 0.5 mM ThT and 10^{-6} M oligonucleotides. The fluorometric output of the G4-dU post-UDG treatment is presented in Fig. 3D and E. These findings demonstrated that untreated G4-dU exhibited fluorescence upon ThT binding, whereas post-UDG treatment resulted in, a marked decreased in fluorescence emission upon G4-dU/ThT complex formation. These observations corroborated the utility of the designed oligonucleotide probe for monitoring UDG enzymatic activity. Furthermore, we explored additional forms of G4-dU by modifying dU at various positions and assessing the fluorescence intensity in combination with ThT after UDG treatment. Our findings (Fig. 3F) suggest that the placement of dU in the loop region at the terminus did not affect fluorescence intensity upon UDG treatment. Conversely, the two alternative modification methods exhibited heightened sensitivity to UDG treatment, leading to notable alterations in fluorescence intensity. In addition, the G-quadruplex can interact with hemin, resulting in the formation of G-quadruplex-hemin nanostructures capable of catalyzing the amplification of chemiluminescence signals in the presence of luminol and H_2O_2. To further support the feasibility of our hypothesis, a similar principle (Fig. 3G) of this property of the G-quadruplex DNA, was used for the detection of UDG through chemiluminescence detection methods. The addition of the UDG enzyme to the detection system resulted in a significant reduction in chemiluminescence compared to that in the control group. (Fig. 3H). These findings corroborate the hypothesis proposed in our methodology.

4. Sensitivity testing

The detection limit of UDG enzyme based on G4-dUw was also tesed. In this study, G4-dU were treated with different

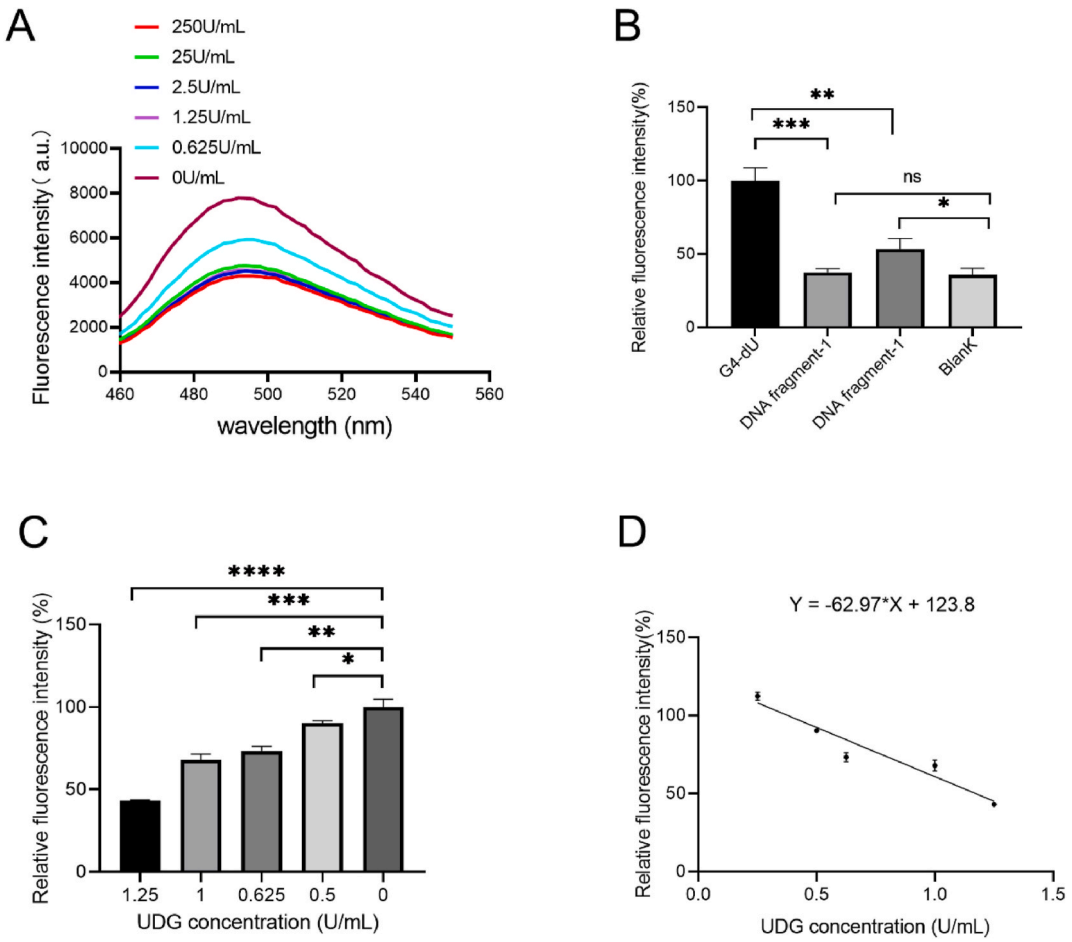

Fig. 4. The impact of varying concentrations of uracil-DNA glycosylase (UDG) enzyme on the efficacy of a detection method.
A. Fluorescence emission spectra of the G4-dU/ThT complex following treatment with varying concentrations of uracil-DNA glycosylase (UDG). B. Analysis of fluorescence intensity of various degraded DNA fragments following incubation with ThT. C Multiple concentrations of UDG were identified, varying from 0U/mL to 1.25U/mL, and standard curve (D) was constructed within this range. The linear equation of the standard curve is $Y = -62.97*X + 123.8$.

concentrations of UDG. As shown in Fig. 4A, the fluorescence intensity of G4-dU treated with 250U/mL to 1.25U/mL of UDG was equivalent, and was significantly lower than that of G4-dU bound to ThT without UDG treatment. When the UDG concentration was reduced to 0.625U/mL, the fluorescence intensity remained lower than that of the G4-dU bound to ThT without UDG treatment. That is, the protocol based on G4-dU detection of the UDG enzyme can detect at least 0.625U/mL of the enzyme.

Upon the addition of 250U/mL UDG, the fluorescence intensity was greater than that of the control. To confirm this observation, we synthesized two degradation products: fragment 1 (GGGGTTTGGGGT) and fragment 2 (GGGGTTTGGGGTTTGGGGT). The subsequent incubation of these fragments with ThT resulted in fluorescence intensity measurements as depicted in Fig. 4B. Notably, the fluorescence intensity remained unchanged upon the incubation of fragment 1 with ThT, whereas fragment 2 exhibited an enhanced line pattern relative to the background fluorescence. This finding further supports the observation that the fluorescence intensity exceeded the background level following the introduction of 250U/mL UDG. To elucidate the detection limit and variability of the novel method, the change in the fluorescence intensity of the G4-dU/ThT complex post UDG treatment was measured across a range of UDG concentrations from 0U/mL to 1.25U/mL (Fig. 4C). A linear correlation was established between the UDG concentration (0–1.25U/mL) and fluorescence intensity (Fig. 4D).

4.1. Screening of UDG inhibitors

UDG activity is selectively inhibited by the uracil glycosylase inhibitor (UGI) protein. The assay developed in this study was aimed at identifying potential UDG antagonists. To validate the assay, variable concentrations of UGI were co-incubated with UDG at different ratios before introduction into a system comprising G4-dU, and subsequent fluorescence monitoring. As shown in Fig. 5AB, the absence of UDG and UGI in the assay milieu resulted in pronounced fluorescence emission. Conversely, the incorporation of UDG alone resulted in minimal fluorescence detection. A progressive increase in the UGI concentration within the UDG-containing environment yielded an incremental fluorescence intensity similar to, that of the UDG-deficient control. These observations corroborated the utility of the constructed assay for identifying UDG inhibitors. The relationship between the concentration of UGI (from 0.1U/mL to 0.6 U/mL) and the relative fluorescence intensity can be expressed as $Y = 2.101*X + 0.5900$, $R^2 = 0.93$ indicating a linear dependence. Based on the 3.3σ principle, the method can detect UGI at a limit of 0.3U/mL.

5. Statistical analysis

Data were analyzed using an unpaired *t*-test in GraphPad Prism 9.5.0 (GraphPad Software Inc., La Jolla, CA, USA)

6. Discussion

The chemotherapeutic agent 5-FU, exerts cytotoxic effects on neoplastic cells by inhibiting of thymidylate synthase, leading to the misincorporation of 5-FU residues instead of thymine within the DNA strand. However, therapeutic resistance is frequently encountered in clinical settings, predominantly due to the cellular expression of UDG, which excises mis-incorporated uracil or 5-FU from the DNA, thereby circumventing the efficacy of the drug. Corroborating this, prognostic evaluations in the current investigation revealed that elevated UNG protein levels were correlated with adverse outcomes in patients with pulmonary carcinoma, reinforcing the hypothesis that UDG inhibition could potentiate the antineoplastic activity of 5-FU. In this study, we employed a uniquely crafted DNA probe sequence to identify UDG inhibitors using a simple design strategy. This study confirmed that the inclusion of deoxyuridine

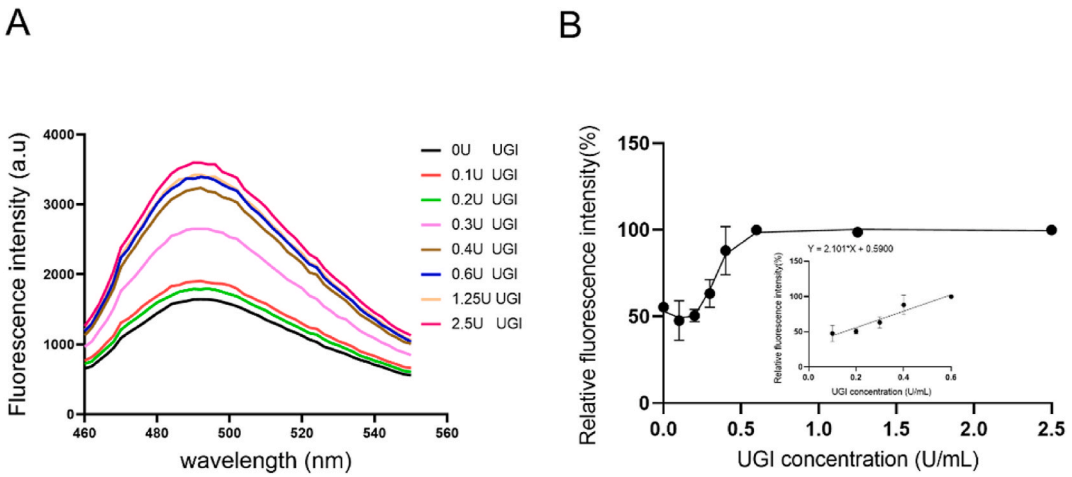

Fig. 5. Activity of UDG after adding different amounts of UGI. The concentration of UDG was 125U/mL.
A. Multiple concentrations of UGI were identified, ranging from 0U/mL to 2.5U/mL. B. A standard curve (from 0.1 U/mL to 0.6U/mL) was constructed within this range. The linear equation of the standard curve is $Y = 2.101*X + 0.5900$.

residues within the G-quadruplex (G4) loop does not compromise its selective affinity for ThT, a feature exploited to facilitate UDG detection and subsequent UGI screening. This novel assay surpassed alternative G4-based methodologies for UDG inhibition owing to its simplicity and independence from auxiliary DNA sequences. Moreover, the absence of enzymatic components such as DNA polymerase, nicking endonucleases, and endonuclease IV in the design precludes the need for an amplification step, enabling the detection of UDG at lower concentrations while minimizing assay interference. This reduces the likelihood of false positives during inhibitor screening. The underlying principle of the assay is that UDG addition disrupts the G4 structure and diminishes fluorescence, ensuring that cellular G4 configurations do not influence the detection outcomes.

Bioinformatic analysis indicated a significant increase in the level of UDG in lung cancer cells, with high expression of this enzyme being detrimental to the prognosis and survival of patients with lung cancer. Furthermore, lung cancer cells serve as viable samples for future detection. Additionally, this method enables the rapid and convenient screening of UDG inhibitors, which can be combined with 5-FU to assess the apoptosis of lung cancer cells following co-administration.

7. Conclusion

We conducted a bioinformatic assessment of UNG expression across various neoplastic cell lines and examined the correlation between UNG levels survival outcomes in patients with pulmonary carcinoma. These findings indicate UNG upregulation in several neoplasms, with a marked increase in pulmonary malignancies. Additionally, survival analysis of patients with pulmonary carcinoma revealed an inverse relationship between elevated UNG expression and patient prognosis.

Compared with other reported methods for detecting UDG, the proposed method offers several notable advantages. First, it eliminates the need for sophisticated and expensive instrumentation, requiring only devices capable of measuring the fluorescence intensity. Second, the design is remarkably straightforward, involving only a single strand of DNA modified with uracil to form the G4 structure. Third, the detection process is highly efficient, with a completion time of only 0.5–1 h. Finally, the method is cost-effective, as it does not require the use of additional enzymes, such as chain replacement DNA polymerase, nicking endonucleases, or endonuclease IV. Therefore, this assay is notably straightforward and expedient, and offer potential as a high-throughput screening technique for UDG inhibitor discovery in future oncological research.

CRediT authorship contribution statement

Pansong Zhang: Writing – original draft, Funding acquisition, Data curation, Conceptualization. **Fangfang He:** Investigation, Formal analysis. **Xin Chang:** Project administration.

Declaration of competing interest

The authors declare that they have no known competing financial interests or personal relationships that could have appeared to influence the work reported in this paper.

Data availability

Data will be made available on request.

Acknowledgments

This work was supported by the PhD Scientific Research Start-Up Fund of Changzhi Medical College (BS202209) and the Science and Technology Innovation Project of Higher Education institutions of Shanxi province (2023L203). Thanks for the instrument platform provided by the Central Laboratory of Changzhi Medical College.

Appendix A. Supplementary data

Supplementary data to this article can be found online at https://doi.org/10.1016/j.heliyon.2024.e37171.

References

[1] J.J. Wyrick, S.A. Roberts, Genomic approaches to DNA repair and mutagenesis, DNA Repair 36 (2015) 146–155, https://doi.org/10.1016/j.dnarep.2015.09.018.

[2] J.M. Daley, C. Zakaria, D. Ramotar, The endonuclease IV family of apurinic/apyrimidinic endonucleases, Mutat. Res. 705 (2010) 217–227, https://doi.org/10.1016/j.mrrev.2010.07.003.

[3] A. Cumova, V. Vymetalkova, A. Opattova, V. Bouskova, B. Pardini, K. Kopeckova, R. Kozevnikovova, K. Lickova, M. Ambrus, L. Vodickova, A. Naccarati, P. Soucek, P. Vodicka, Genetic variations in 3'UTRs of SMUG1 and NEIL2 genes modulate breast cancer risk, survival and therapy response, Mutagenesis 36 (2021) 269–279, https://doi.org/10.1093/mutage/geab017.

[4] J.A. van Laar, Y.M. Rustum, S.P. Ackland, C.J. van Groeningen, G.J. Peters, Comparison of 5-fluoro-2ˈ-deoxyuridine with 5-fluorouracil and their role in the treatment of colorectal cancer, Eur. J. Cancer 34 (1998) 296–306, https://doi.org/10.1016/s0959-8049(97)00366-3.
[5] D.B. Longley, D.P. Harkin, P.G. Johnston, 5-fluorouracil: mechanisms of action and clinical strategies, Nat. Rev. Cancer 3 (2003) 330–338, https://doi.org/10.1038/nrc1074.
[6] S. Vodenkova, T. Buchler, K. Cervena, V. Veskrnova, P. Vodicka, V. Vymetalkova, 5-fluorouracil and other fluoropyrimidines in colorectal cancer: past, present and future, Pharmacol. Ther. 206 (2020) 107447, https://doi.org/10.1016/j.pharmthera.2019.107447.
[7] Y. Yan, X. Han, Y. Qing, A.G. Condie, S. Gorityala, S. Yang, Y. Xu, Y. Zhang, S.L. Gerson, Inhibition of uracil DNA glycosylase sensitizes cancer cells to 5-fluorodeoxyuridine through replication fork collapse-induced DNA damage, Oncotarget 7 (2016) 59299–59313, https://doi.org/10.18632/oncotarget.11151.
[8] M.T. Nguyen, D. Moiani, Z. Ahmed, A.S. Arvai, S. Namjoshi, D.S. Shin, Y. Fedorov, E.J. Selvik, D.E. Jones, J. Pink, Y. Yan, D.J. Laverty, Z.D. Nagel, J.A. Tainer, S. L. Gerson, An effective human uracil-DNA glycosylase inhibitor targets the open pre-catalytic active site conformation, Prog. Biophys. Mol. Biol. 163 (2021) 143–159, https://doi.org/10.1016/j.pbiomolbio.2021.02.004.
[9] E.S. Christenson, A. Gizzi, J. Cui, M. Egleston, K.J. Seamon, M. DePasquale, B. Orris, B.H. Park, J.T. Stivers, Inhibition of human uracil DNA glycosylase sensitizes a large fraction of colorectal cancer cells to 5-fluorodeoxyuridine and raltitrexed but not fluorouracil, Mol. Pharmacol. 99 (2021) 412–425, https://doi.org/10.1124/molpharm.120.000191.
[10] Y. Li, S. Xu, X. Wu, Q. Xu, Y. Zhao, X. Lou, X. Yang, Thioflavin T as a fluorescence light-up probe for both parallel and antiparallel G-quadruplexes of 29-mer thrombin binding aptamer, Anal. Bioanal. Chem. 408 (2016) 8025–8036, https://doi.org/10.1007/s00216-016-9901-5.
[11] A. Renaud de la Faverie, A. Guedin, A. Bedrat, L.A. Yatsunyk, J.L. Mergny, Thioflavin T as a fluorescence light-up probe for G4 formation, Nucleic Acids Res. 42 (2014) e65, https://doi.org/10.1093/nar/gku111.
[12] Y.C. Du, L.N. Zhu, D.M. Kong, Label-free thioflavin T/G-quadruplex-based real-time strand displacement amplification for biosensing applications, Biosens. Bioelectron. 86 (2016) 811–817, https://doi.org/10.1016/j.bios.2016.07.083.
[13] L. Dong, X. Zhang, Y. Li, F. E, J. Zhang, Y. Cheng, Highly sensitive detection of uracil-DNA glycosylase activity based on self-initiating Multiple rolling circle amplification, ACS Omega 4 (2019) 3881–3886, https://doi.org/10.1021/acsomega.8b03376.
[14] E. Tan, B. Erwin, S. Dames, T. Ferguson, M. Buechel, B. Irvine, K. Voelkerding, A. Niemz, Specific versus nonspecific isothermal DNA amplification through thermophilic polymerase and nicking enzyme activities, Biochemistry 47 (2008) 9987–9999, https://doi.org/10.1021/bi800746p.
[15] G. Luo, H. He, D. Wang, S. Liu, S. Tian, M. Chen, Q. Wang, C. Zhao, Z. Leng, L. Hou, X. Guo, Tandem repeat generation and novel isothermal amplification based on nonspecific tailing and replication slippage, Clin. Chem. 69 (2023) 363–373, https://doi.org/10.1093/clinchem/hvac199.
[16] X. Liang, K. Jensen, M.D. Frank-Kamenetskii, Very efficient template/primer-independent DNA synthesis by thermophilic DNA polymerase in the presence of a thermophilic restriction endonuclease, Biochemistry 43 (2004) 13459–13466, https://doi.org/10.1021/bi0489614.
[17] F. Jiao, P. Qian, Y. Qin, Y. Xia, C. Deng, Z. Nie, A novel and label-free biosensors for uracil-DNA glycosylase activity based on the electrochemical oxidation of guanine bases at the graphene modified electrode, Talanta 147 (2016) 98–102, https://doi.org/10.1016/j.talanta.2015.09.045.
[18] H. Zhao, W. Hu, J. Jing, X. Zhang, One-step G-quadruplex-based fluorescence resonance energy transfer sensing method for ratiometric detection of uracil-DNA glycosylase activity, Talanta 221 (2021) 121609, https://doi.org/10.1016/j.talanta.2020.121609.
[19] G. Li, S.A. Henry, H. Liu, T.S. Kang, S.C. Nao, Y. Zhao, C. Wu, J. Jin, J.T. Zhang, C.H. Leung, P. Wai Hong Chan, D.L. Ma, A robust photoluminescence screening assay identifies uracil-DNA glycosylase inhibitors against prostate cancer, Chem. Sci. 11 (2020) 1750–1760, https://doi.org/10.1039/c9sc05623h.